Amino Acids (2015) 47:1239–1246
DOI 10.1007/s00726-015-1950-0

ORIGINAL ARTICLE

Targeting rho guanine nucleotide exchange factor ARHGEF5/TIM with auto-inhibitory peptides in human breast cancer

Ou Huang · Dandan Wu · Feiyan Xie · Lili Lin · Xiaobo Wang · Min Jiang · Yafen Li · Weiguo Chen · Kunwei Shen · Xiaoqu Hu

Received: 26 September 2014 / Accepted: 23 February 2015 / Published online: 6 March 2015

Abstract The oncogenic protein ARHGEF5/TIM has long been known to express specifically in human breast cancer and other tumors, which is an important member of Rho guanine nucleotide exchange factors that activate Rho-family GTPases by promoting GTP/GDP exchange. The activation capability of TIM is auto-inhibited by a putative helix N-terminal to Dbl homology (DH) domain, which is stabilized by intramolecular interaction of Src homology 3 domain with a poly-proline sequence that locates between the helix and DH domain. Here, we attempted to target TIM DH domain using the modified versions of its auto-inhibitory helix. In the procedure, bioinformatics techniques were used to investigate the intramolecular interaction of DH domain with auto-inhibitory helix and, based on obtained knowledge, to optimize physicochemical property and structural conformation for the helix. We also performed affinity assay to determine the binding strength of modified peptides to DH domain. Consequently, two modified peptides, namely, DALYEEYNLVV and EVLYEEYQLVV were found as good binders of DH domain with dissociation constants K_d of 0.35 and 2 μM, respectively. Structural analysis revealed that the charge neutralization and electrostatic interaction confer additional stability for these two peptide complexes with DH domain.

Keywords ARHGEF5/TIM · DH domain · Auto-inhibitory helix · Peptide · Breast cancer

Handling Editor: M. S. Palma.

O. Huang · Y. Li · W. Chen · K. Shen
Department of Surgery, Ruijin Hospital, Medical School of Shanghai Jiaotong University, Shanghai 200025, China

D. Wu
International Peace Maternity and Child Health Hospital, Shanghai Jiaotong University, Shanghai 200023, China

F. Xie · L. Lin · X. Wang · X. Hu (✉)
Department of Surgical Oncology, The First Affiliated Hospital of Wenzhou Medical University, Wenzhou, Zhejiang 325000, China
e-mail: drhxj@126.com

M. Jiang
Department of Breast Surgery, The First Affiliated Hospital of Soochow University, Suzhou 215006, China

Introduction

Rho-family GTPases are molecular switches that control a wide variety of signal transduction pathways in all eukaryotic cells (Etienne-Manneville and Hall 2002), which are directly regulated by Rho guanine nucleotide exchange factors (RhoGEFs) in response to diverse extracellular stimuli, and ultimately regulate diverse cellular behaviors such as proliferation, differentiation and movement (Rossman et al. 2005). RhoGEFs represent a large family of complex proteins with numerous signaling domains, but they almost invariably contain a functional tandem, including a Dbl homology (DH) domain responsible for guanine nucleotide exchange, followed by a Pleckstrin homology (PH) domain, which targets the GEF to the plasma membrane and/or regulates nucleotide exchange (Chhatriwala et al. 2007).

The Rho guanine nucleotide exchange factor 5 (ARHGEF5) is an important member of RhoGEF family that regulates cell adhesion and migration as well as extracellular matrix remodeling in normal and cancer cells by participating in Src-induced podosome formation (Kuroiwa et al. 2011). The ARHGEF5 has a short isoform known as TIM, which is an oncogenic protein corresponding to the

C-terminal 519 amino acids of ARHGEF5. The TIM was found to play a crucial role in the tumorigenesis and metastasis of various tumors (Barrio-Real and Kazanietz 2012), which has long been identified as a potential therapeutic target of human breast cancer (Debily et al. 2004). Previously, Bouquier et al. performed high-throughput screening of peptide aptamers as potent inhibitors to interfere with RhoGEF functions (Bouquier et al. 2009). Very recently, He et al. (2015) obtained several SH3-binding peptides capable of promoting TIM-catalyzed exchange activity. All these works suggested that it is feasible of designing peptide ligands to target TIM for breast cancer therapy.

An important feature of RhoGEF family members is the auto-inhibition, that is, the catalytic activity of PH domain can be inhibited by intramolecular interactions between different domains and/or different segments within a single RhoGEF protein (Schiller et al. 2006). This feature is also applicable for TIM. Besides DH and PH domains, TIM possesses an additional SH3 domain at its C-terminus. The activation capability of TIM is auto-inhibited by a putative helix N-terminal to DH domain, which is stabilized by intramolecular interaction of the SH3 domain with a polyproline sequence that locates between the helix and DH domain (Yohe et al. 2007, 2008). Here, we reported successful application of combining bioinformatics analysis and wet-lab experiment to rationally design peptide binders of TIM DH domain using the auto-inhibitory helix as starting point. In the procedure, bioinformatics techniques were used to investigate the intramolecular interaction of DH domain with auto-inhibitory helix and, based on obtained knowledge, to optimize the physicochemical property and structural conformation for the helix, aiming at obtaining a number of modified auto-inhibitory peptides with high affinity and specificity to competitively target DH domain. We also performed fluorescence spectroscopic analysis to solidify the findings arising from theoretical study. Furthermore, the structural basis, energetic property and biological implication underlying the interaction between the DH domain and designed auto-inhibitory peptides were examined in detail. This study can be regarded as a successful application of computational peptidology proposed recently by Zhou et al. (2013) in rational peptide design.

Materials and methods

DH domain modeling and auto-inhibitory helix folding

Since the high-resolution structure data of either complete TIM protein or its separated domains are still unavailable, we therefore employed bioinformatics approach to computationally model the atomic structures of DH domain and auto-inhibitory helix.

The primary sequence of TIM DH domain (corresponding to the amino acids 1174–1358 of ARHGEF5 protein in the UniProt database (Uniprot 2010) with accession ID Q12774) was searched against the entire PDB database (Berman et al. 2000) and, consequently, the DH domain of ARHGEF11 was found as the best target protein with sequence similarity score 36.7 %. Thus, homology modeling method was applied to predicting TIM DH structure from the crystal template of ARHGEF11 DH domain (PDB: 1XCG). Here, the SWISS-MODEL server (Schwede et al. 2003) was used to automatically fulfill the homology modeling procedure, which included three successive steps of conserved structure grafting, loop region optimization and global annealing refinement, resulting in the refined structure model of TIM DH domain.

The auto-inhibitory helix locates at N-terminal region of TIM protein and precedes DH domain, which was supposed to form a well-defined α-helix and roots against the active site of the domain (Yohe et al. 2007, 2008). The helix contains a core heptapeptide motif (LYQEYSD, amino acids 1096–1102 of ARHGEF5) capped by two extended amino acids at each side (*QL*LYQEYSD*VV*). The helical folding mode was predicted using de novo PEP-FOLD server (Maupetit et al. 2009) from its primary sequence of the 11-mer peptide (core + extension), which was subsequently imposed with molecular mechanism minimization to relax the artificial structure model.

Molecular docking and complex refinement

Since no global docking strategies are available to date for blindly modeling protein–peptide interaction, the protein docking method ZDOCK (Pierce et al. 2014) was employed here to perform coarse-grained search for the binding modes of auto-inhibitory helical peptide to TIM DH domain. The ZDOCK has been widely used in bioinformatics community to predict the complex systems of protein with protein, nucleic acid and peptide, which considers shape complementarity as well as solvent effect and electrostatic factor to fast match two docked components; benchmark test showed that the method performed fairly well for most biomolecular systems in different conditions (Chen et al. 2003). Before protein–peptide docking, hydrogen atoms were added to peptide structures and protonation state was assigned for the ionizable residues (such as Arg and Glu) using WHAT IF server (Vriend 1990). The docked complex structure models of TIM DH domain with helical peptide were further refined in a computationally expensive manner with FlexPepDock server (London et al. 2011), which combined Monte Carlo sampling and Rosetta force field to minimize the structure for the protein–peptide system to achieve their global energy minimum, resulting

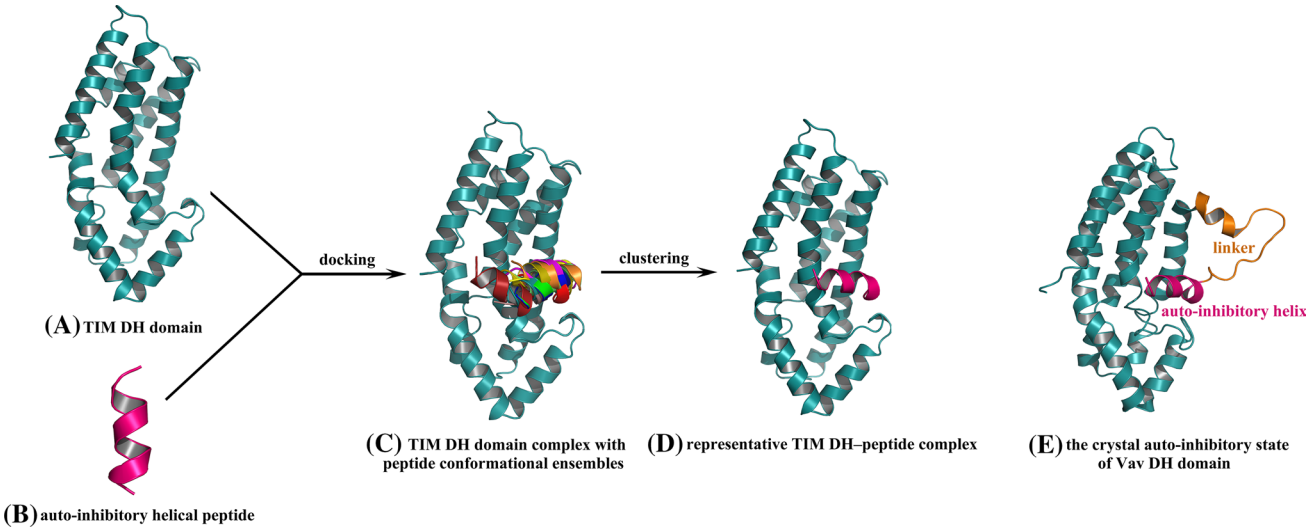

Fig. 1 Schematic representation of modeling DH domain–auto-inhibitory complex. The three-dimensional structures of TIM DH domain (**a**) and auto-inhibitory helical peptide (**b**) were folded using homology modeling and de novo prediction approaches, respectively. They were then docked to each other to generate conformational ensembles of peptide ligand in the active site of DH domain (**c**), which were further clustered into a single representative DH–peptide complex structure model (**d**). For comparison purpose, the crystal auto-inhibitory state of Vav DH domain, where the auto-inhibitory helix is connected to DH domain via a loop linker (PDB: 1F5X)

in multiple conformational ensembles for the system, which can be clustered into a representative model.

Molecular dynamics simulation and free energy analysis

The molecular dynamics (MD) simulations were performed with AMBER03 force field (Duan et al. 2003). In brief, the modeled complex structure of TIM DH domain with peptide ligand was solvated in an implicit water environment. The Particle Mesh Ewald (PME) method (Darden et al. 1993) was used to calculate the full electrostatic energy of a unit cell in a macroscopic lattice of repeating images, and SHAKE algorithm (Ryckaert et al. 1977) was employed to constrain all hydrogen atoms in system. The simulation consisted of a gradual temperature increase from 10 to 298 K over 1 ns and a 10-ns production phase for data collection; the dynamics trajectory was saved every 100 ps. The snapshots saved during the production phase were utilized to perform free energy analysis of peptide binding to TIM DH domain using molecular mechanics/Poisson–Boltzmann surface area (MM-PB/SA) method (Kollman et al. 2000).

Binding affinity assay

The fluorescence emission spectra of tryptophan residues in the domain were used to monitor the changes in structural environment of the tryptophan upon peptide binding (Liu et al. 2014). Fluorescence was measured by a Perkin-Elmer fluorescence spectrophotometer. The protein concentration was kept at a constant. Changes in fluorescence were measured upon titration of peptide solution. Peptide affinity K_d (dissociation constant) was obtained by fitting experimental data to equation $F = [F_0 + F_\infty([p]/Kd)]/[1 + ([p]/K_d)]$, where [p] is the final peptide concentration at each measurement point, F is the measured protein fluorescence intensity of TIM DH domain at the particular peptide concentration, F_0 is intensity in the absence of peptide ligand, and F_∞ is the observed maximal fluorescence intensity of the protein when saturated with the peptide.

Results and discussions

Structural modeling of DH domain–auto-inhibitory helix complex

To understand the atomic details of intramolecular interaction between the DH domain and auto-inhibitory helix within TIM protein, a computational protocol was applied to modeling the complex structure of DH domain with auto-inhibitory helical peptide (Fig. 1a–d). First, the three-dimensional structures of DH domain and auto-inhibitory helix were folded using homology modeling and de novo prediction approaches, respectively. They were then docked to each other to generate conformational ensembles of peptide ligand in the active site of DH domain, which were further clustered into a single representative DH–peptide complex structure model. As can be seen, the TIM DH domain is composed of seven α-helices to form a typical all-alpha

protein (Fig. 1a) according to the SCOP protein structure classification (Hubbard et al. 1999). The catalytic pocket is a depressed region at one side of the protein that is evolved to accommodate Rho GTPase substrate and, alternatively, blocked by auto-inhibitory helix (Fig. 1b). The molecular docking generated multiple conformations of helical peptide within the pocket (Fig. 1c); they can be regarded as potential binding modes of the peptide in different microstates (Baysal and Meirovitch 1997). Clustering analysis further revealed a representative mode that is a time average of these conformations (Fig. 1d) and will be used in subsequent analysis to investigate the structural basis and energetic property of auto-inhibitory helix binding to DH domain.

For comparison purpose, the crystal auto-inhibitory state of Vav DH domain is shown in Fig. 1e. The Vav protein is also a Dbl member that acts as guanine nucleotide exchange factor for small G proteins of the Rho family, which behaves auto-inhibition through a N-terminal helix connected to DH domain via a loop linker. These features make Vav very similar to TIM in structure and function, demonstrating that the computationally modeled binding mode of helical peptide to TIM DH domain is highly reliable as it shares high structural conservation with the auto-inhibitory Vav DH domain determined by crystallographic approach, although we herein did not consider the linker that is actually also existed between the DH domain and auto-inhibitory helix of TIM protein. In fact, according to the self-inhibitory peptide theory published recently by Yang et al. (2015), the linker should not address substantial effect on the domain–helix interaction due to its high flexibility and structural independency.

It is evident from Fig. 2a that the contact region with auto-inhibitory helix is at the depressed center of TIM DH domain and packs tightly against the helix that is about perpendicular to the arrangement of DH seven-helical bundle. Structural examination characterized intensive nonbonded interactions at the domain–helix contact interface (Zhou et al. 2012). As can be seen in Fig. 2b, a number of van der Waals and hydrophobic forces are observed across the interface, conferring high stability for the auto-inhibitory complex architecture. In addition, the helix can form three geometrically satisfactory hydrogen bonds with the residues Ser135, Arg143 and Thr145 of DH domain, which guarantee specificity and selectivity for the domain–helix recognition. Binding free energy calculation further revealed a high affinity of $\Delta G_{\text{total}} = -16.2$ kcal/mol associated with the domain–helix binding, which can be decomposed into direct nonbonded interaction of $\Delta G_{\text{nonbonded}} = -132.4$ kcal/mol and indirect desolvation penalty of $\Delta G_{\text{desolvation}} = 116.2$ kcal/mol, suggesting that the binding is an exquisite balance between favorable nonbonded force and unfavorable solvent effect. In this respect, we should address structure modification on the helical peptide to improve the favorable nonbonded force and simultaneously minimize the unfavorable solvent effect, while keeping its intrinsically helical conformation.

Rational optimization of auto-inhibitory helical peptide

Here, we attempted to optimize the sequence pattern of auto-inhibitory helical peptide based on its modeled complex structure with DH domain. First, key residues in the peptide were identified that would be kept invariably in the optimization procedure. The key residues were considered as those that can form definite nonbonded interactions with DH domain and/or contribute significantly to peptide affinity. As described above, the peptide residues Tyr4, Glu6 and Tyr7 were suggested as key residues since they can separately form three hydrogen bonds with the domain; these hydrogen bonds were thought to play a critical role in constituting specificity and selectivity for domain–helix recognition. In addition, the Tyr4 and Tyr7 were also observed to participate in cation–π interactions with Arg146 and Arg143 of DH domain, respectively.

Further, we employed virtual alanine scanning technique (Kortemme et al. 2004) to determine the independent affinity contributions of peptide residues, that is, each of the 11 peptide residues in auto-inhibitory helix was separately mutated in silico to the neutral alanine and then evaluated mutation effect on helical peptide's affinity to DH domain. Here, the virtual mutation was carried out using SCAP program (Xiang and Honig 2001), and the binding free energy change ($\Delta\Delta G_{\text{mutation}}$) upon mutation can be calculated as the difference between the total binding free energies (ΔG_{total}) of mutated and unmutated peptides to the domain, viz. $\Delta\Delta G_{\text{mutation}} = \Delta G_{\text{total}}^{\text{mutated}} - \Delta G_{\text{total}}^{\text{unmutated}}$. Consequently, a systematic profile of virtual alanine scanning against the 11-mer helical peptides was obtained; it can be visualized as a histogram in Fig. 3. As might be expected, the key residues Tyr4, Glu6 and Tyr7 defined above were characterized to be essential in domain–peptide interaction due to a large free energy loss ($\Delta\Delta G_{\text{mutation}} > 0.9$ kcal/mol) upon mutation of them to alanine. In addition, the two C-terminal residues Val10 and Val11 as well as the residue Leu3 seem to also contribute considerably to peptide affinity with $\Delta\Delta G_{\text{mutation}} > 0.5$ kcal/mol. Visualization analysis of domain–peptide complex structure revealed that these three nonpolar residues locate at one side of auto-inhibitory helix and pack tightly against DH domain (Fig. 4); the packing is involved with intensive van der Waals and hydrophobic contacts. In this regard, we also defined the Leu3, Val10 and Val11 as key residues for domain–peptide interaction.

According to above analysis, peptide residues Leu3, Tyr4, Glu6, Tyr7, Val10 and Val11 are considered as the key residues that play an essential role in stabilizing

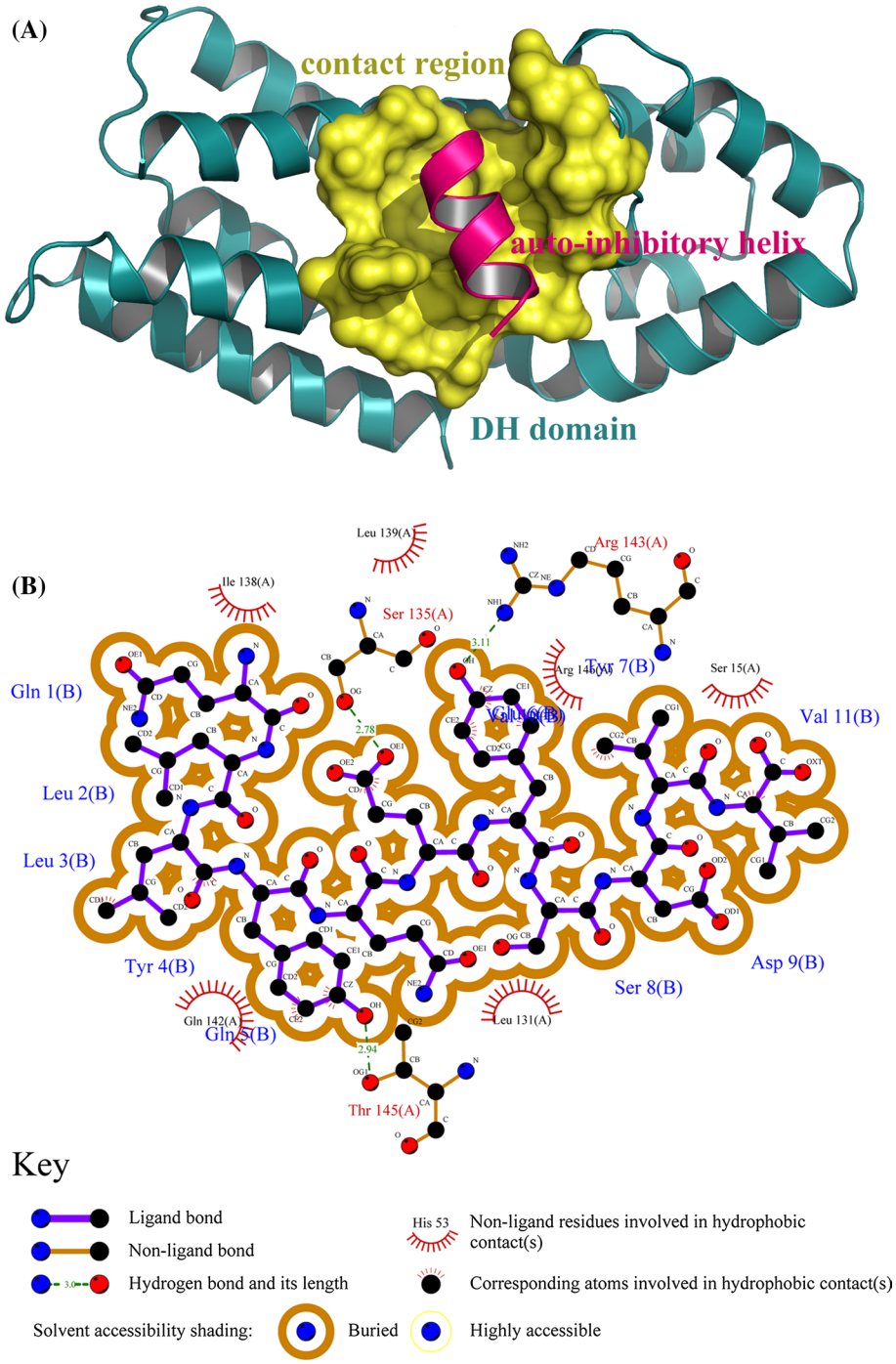

Fig. 2 **a** The contact region with auto-inhibitory helix in TIM DH domain. **b** Schematic representation of nonbonded interactions across the contact interface of TIM DH domain with auto-inhibitory helix. There are three hydrogen bonds and a number of van der Waals and hydrophobic forces at the interface to confer stability and specificity for the complex architecture. This plot was generated using LIGPLOT program (Wallace et al. 1995)

domain–peptide complex architecture. Thus, they were fixed in peptide optimization procedure, while the amino acid types of other five residue positions, i.e., Gln1, Leu2, Gln5, Ser8 and Asp9, were optimized in a high-throughput manner, aiming at a further improvement of helical peptide affinity to DH domain. In the procedure, virtual mutagenesis was carried out to derive systemic mutants at each of the five residues. According to a strategy described by Hou et al. (2006), systematic single-point mutation was carried out on the native helical peptide in complex with DH domain; each of the five residues was one-by-one mutated to other 19 amino acid types using SCAP program (Xiang and Honig 2001), followed by a force field minimization procedure to relax the mutated complex system. Consequently, a total of $5 \times 19 = 95$ peptide single-point mutants plus the native one were obtained. Based on binding free energy analysis of native peptide and its mutants to DH domain, we defined a 5×19 matrix to describe the

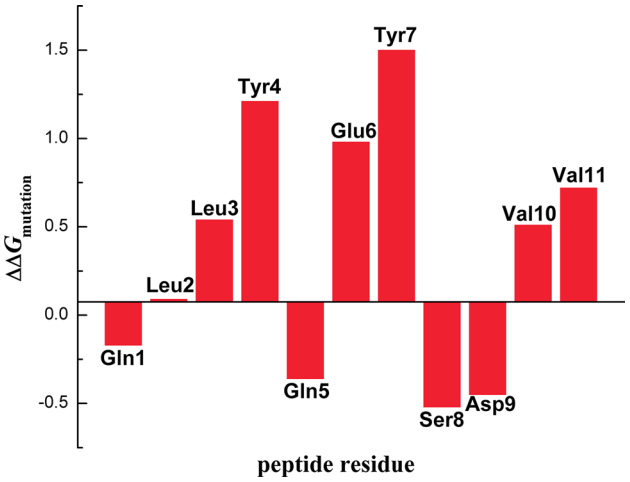

Fig. 3 The binding free energy change profile of peptide residue mutations calculated by virtual alanine scanning and binding energy analysis

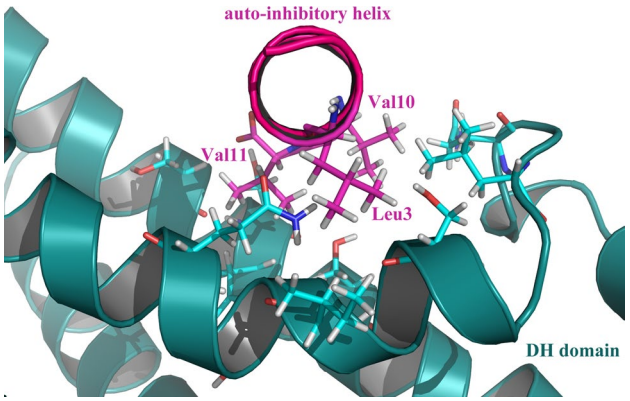

Fig. 4 The two C-terminal residues Val10 and Val11 as well as residue Leu3 of helical peptide locate at one side of the auto-inhibitory helix and pack tightly against DH domain

free energy change profile upon systematic mutations at the five non-key residue positions (Fig. 5); element $m(i,j)$ of the matrix represents domain–peptide binding free energy change $\Delta\Delta G_{\text{mutation}}$ upon mutation of peptide residue i to amino acid type j ($i = 1, 2, 3, 4, 5$; $j = 1, 2, 3, \ldots, 19$). In this way, we can obtain the favorable ($\Delta\Delta G_{\text{mutation}} < 0$) and unfavorable ($\Delta\Delta G_{\text{mutation}} > 0$) amino acid types at each peptide position relative to native residue.

It is evident from Fig. 5 that most mutations show to have only a modest effect on domain–peptide binding affinity ($|\Delta\Delta G_{\text{mutation}}| < 1$ kcal/mol); this is not unexpected since the five residues do not participate in strong interactions with DH domain so that mutations of them are likely to be neutral for most cases. However, few mutations can address significant effect on peptide binding with $\Delta\Delta G_{\text{mutation}} < -1$ kcal/mol (favorable) or > 1 kcal/mol (unfavorable) that are considered as hotspot substitutions and are particularly interested in this study. As can be seen, these hotspots are concentrated in those charged (e.g., Arg, Asp and Glu) or aromatic, bulky (e.g., Tyr and Trp) amino acids, while many small amino acids such as Gly, Cys and Ser tend to play a neutral role in the mutation. Here, we only concerned favorable mutations for each of the five non-key residues, that is, Asp and Glu for residue 1, Ala, Val and Pro for residue 2, Tyr and Glu for residue 5, Asn and Gln for residue 8, and Ile and Leu for residue 9. Interestingly, favorable mutations are likely to be conserved for a given residue position, for example, the Asp and Glu at residue 1, the Ala and Val at residue 2, and the Asn and Gln at residue 8. This is not unexpected if considering that the conserved amino acids share similar physicochemical, structural and biological properties that can exert a homogeneous effect on peptide binding at the same residue position.

According to above analysis, the residue positions 1, 2, 5, 8 and 9 have 2 (Asp and Glu), 3 (Ala, Val and Pro), 2 (Tyr and Glu), 2 (Asn and Gln) and 2 (Ile and Leu) favorable amino acid types, respectively, and they can generate totally 48 ($2 \times 3 \times 2 \times 2 \times 2$) combinations, which were considered as candidate peptides modified from native auto-inhibitory helix (Fig. 6). Moreover, considering that helicity is essential for high-affinity binding of helical peptide to DH domain, we herein employed PEP-FOLD server (Maupetit et al. 2009) to predict folded structures for the 48 candidate peptides, and used DSSP tool (Kabsch and

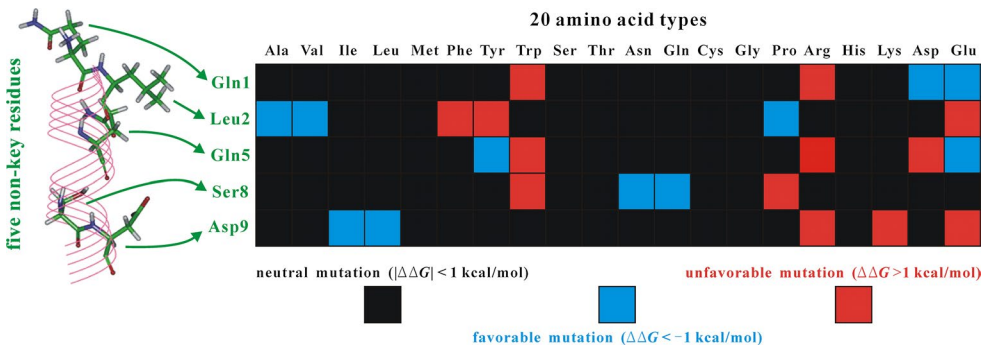

Fig. 5 The free energy change profile upon systematic mutations at the five non-key residues of helical peptide

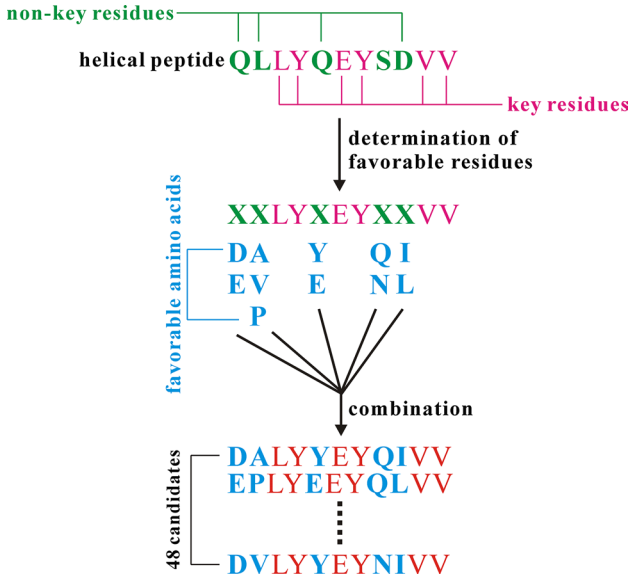

Fig. 6 Schematic representation of determining favorable amino acids at the five non-key residues of helical peptide and combining these favorable amino acids to result in 48 modified peptide candidates

Table 1 The six promising peptides modified from native helical peptide

Peptide	Helicity (%)	ΔG_{total} (kcal/mol)	K_d (μM)
QLLYQEYSDVV[a]	81.8	−16.2	12
DALYEEYNLVV	72.7	−18.0	0.35
DVLYYEYQLVV	72.7	−17.4	56
DALYYEYNIVV	72.7	−17.2	120
DPLYEEYQIVV	90.9	−16.9	nd
EVLYEEYQLVV	72.7	−17.8	2
EPLYYEYNIVV	90.9	−16.5	nd

nd not determined

[a] Native helical peptide

Sander 1983) to analyze the helicity of these peptides based on their predicted structures. As a result, 15 out of the 48 peptides were inferred to be highly helixicated, with helicity ≥72.7 % (viz. 8 or more residues in the 11-mer peptide were assigned as helical residues). Next, the 15 peptide complexes with DH domain were modeled from domain–native peptide structure using virtual mutagenesis strategy, and free energy analysis based on MD simulations was then carried out on the modeled complexes to characterize the binding affinity of these peptides to DH domain. Consequently, six modified peptides were predicted to have an increased affinity due to mutations, and their information is listed in Table 1 for comparison purpose. To solidify the findings derived from computational analysis, fluorescence spectroscopy assay was performed to determine the binding affinities of six modified peptides as well the native one to DH domain and, consequently, four out of the six peptides were measured to have moderate or high affinity. In particular, the modified mutants DALYEEYNLVV and EVLYEEYQLVV were found as stronger binders of DH domain with K_d values of 0.35 and 2 μM, which are lower than that of native peptide (K_d = 12 μM). These high-affinity peptides possess a negatively charged Asp or Glu at their N-terminus that is able to neutralize and, thus, stabilize the N-terminal positive charge of peptide. In addition, the negatively charged Glu at peptide residue 5 was found to form long-range electrostatic interactions with the Arg143 and Arg146 residues of DH domain, which were thought to contribute additional stabilization energy for domain–peptide interaction. Therefore, it is suggested that diverse physicochemical factors co-determine the high affinity of these modified peptides. However, the binding capability of DPLYEEYQIVV and EPLYYEYNIVV were not detectable, albeit they were predicted as good binders of DH domain. The two peptides have a common proline at residue 2, which may cause significant allosteric effect on peptide structure and thus prevent it from binding state owing to the intrinsic conformation constraint of proline.

Acknowledgments This work was supported by the National Natural Science Foundation of China (Nos. 30801118, 81172520, 81202087, 81202088, 81472462 and 81402176), the Natural Science Foundation of Shanghai Municipal Science and Technology Commission (No. 12ZR1446400), the Technology Innovation Act Plan of Shanghai Municipal Science and Technology Commission (Nos. 14411950200 and 14411950201), the Wenzhou Science and Technology Bureau (No. Y20130090), the Natural Science Foundation of Jiangsu Province (No. BK20140288), the Natural Science Foundation of Jiangsu Higher Education Institutions of China (No. 14KJB320011), and the Joint Research Project of the Emerging Cutting-edge Technology of Shanghai Shen-kang Hospital Development Center (No. SHDC12014103).

Conflict of interest The authors declare that they have no conflict of interest.

References

Barrio-Real L, Kazanietz MG (2012) Rho GEFs and cancer: linking gene expression and metastatic dissemination. Sci Signal 5:pe43

Baysal C, Meirovitch H (1997) Determination of the stable microstates of a peptide from NOE distance constraints and optimization of atomic solvation parameters. J Am Chem Soc 114:4805–4818

Berman HM, Westbrook J, Feng Z, Gilliland G, Bhat TN, Weissig H, Shindyalov IN, Bourne PE (2000) The protein data bank. Nucleic Acids Res 28:235–242

Bouquier N, Fromont S, Zeeh JC, Auziol C, Larrousse P, Robert B, Zeghouf M, Cherfils J, Debant A, Schmidt S (2009) Aptamer-derived peptides as potent inhibitors of the oncogenic RhoGEF Tgat. Chem Biol 16:391–400

Chen R, Li L, Weng Z (2003) ZDOCK: an initial-stage protein-docking algorithm. Proteins 52:80–87

Chhatriwala MK, Betts L, Worthylake DK, Sondek J (2007) The DH and PH domains of Trio coordinately engage Rho GTPases for their efficient activation. J Mol Biol 368:1307–1320

Darden T, York D, Pedersen L (1993) Particle mesh Ewald and N.log(N) method for Ewald sums in large systems. J Chem Phys 98:10089–10092

Debily MA, Camarca A, Ciullo M, Mayer C, Marhomy S, Ba I, Jalil A, Anzisi A, Guardiola J, Piatier-Tonneau D (2004) Expression and molecular characterization of alternative transcripts of the ARHGEF5/TIM oncogene specific for human breast cancer. Hum Mol Genet 13:323–334

Duan Y, Wu C, Chowdhury S, Lee MC, Xiong GM, Zhang W (2003) A point-charge force field for molecular mechanics simulations of proteins based on condensed-phase quantum mechanical calculations. J Comput Chem 24:1999–2012

Etienne-Manneville S, Hall A (2002) Rho GTPases in cell biology. Nature 420:629–635

He P, Tan DL, Liu HX, Lv FL, Wu W (2015) The auto-inhibitory state of Rho guanine nucleotide exchange factor ARHGEF5 can be relieved by targeting its SH3 domain with rationally designed peptide aptamers. Biochimie 111:10–18

Hou T, Chen K, McLaughlin WA, Lu B, Wang W (2006) Computational analysis and prediction of the binding motif and protein interacting partners of the Abl SH3 domain. PLoS Comput Biol 2:e1

Hubbard TJ, Ailey B, Brenner SE, Murzin AG, Chothia C (1999) SCOP: a structural classification of proteins database. Nucleic Acids Res 27:254–256

Kabsch W, Sander C (1983) Dictionary of protein secondary structure: pattern recognition of hydrogen-bonded and geometrical features. Biopolymers 22:2577–2637

Kollman PA, Massova I, Reyes C, Kuhn B, Huo SH (2000) Calculating structures and free energies of complex molecules: combining molecular mechanics and continuum models. Acc Chem Res 33:889–897

Kortemme T, Kim DE, Baker D (2004) Computational alanine scanning of protein–protein interfaces. Sci STKE 2004:pl2

Kuroiwa M, Oneyama C, Nada S, Okada M (2011) The guanine nucleotide exchange factor Arhgef5 plays crucial roles in Src-induced podosome formation. J Cell Sci 124:1726–1738

Liu HM, Li LJ, Guo J, Yang ZJ, Yang X, Qi RP, Cao W (2014) Evolution of high-affinity peptide probes to detect the SH3 domain of cancer biomarker BCR-ABL. Int J Pept Res Ther 20:201–208

London N, Raveh B, Cohen E, Fathi G, Schueler-Furman O (2011) Rosetta FlexPepDock web server—high resolution modeling of peptide–protein interactions. Nucleic Acids Res 39:249–253

Maupetit J, Derreumaux P, Tuffery P (2009) PEP-FOLD: an online resource for de novo peptide structure prediction. Nucleic Acids Res 37:W498–W503

Pierce BG, Wiehe K, Hwang H, Kim BH, Vreven T, Weng Z (2014) ZDOCK server: interactive docking prediction of protein–protein complexes and symmetric multimers. Bioinformatics 30:1771–1773

Rossman KL, Der CJ, Sondek J (2005) GEF means go: turning on RHO GTPases with guanine nucleotide-exchange factors. Nat Rev Mol Cell Biol 6:167–180

Ryckaert J, Ciccotti G, Berendsen HJC (1977) Numerical-integration of Cartesian equations of motion of a system with constraints: molecular dynamics of *n*-alkanes. J Comput Phys 23:327–341

Schiller MR, Chakrabarti K, King GF, Schiller NI, Eipper BA, Maciejewski MW (2006) Regulation of RhoGEF activity by intramolecular and intermolecular SH3 domain interactions. J Biol Chem 281:18774–18786

Schwede T, Kopp J, Guex N, Peitsch MC (2003) SWISS-MODEL: an automated protein homology-modeling server. Nucleic Acids Res 31:3381–3385

Uniprot C (2010) Ongoing and future developments at the Universal Protein Resource. Nucleic Acids Res 39:D214–D219

Vriend G (1990) WHAT IF: a molecular modeling and drug design program. J Mol Graph 8:52–56

Wallace AC, Laskowski RA, Thornton JM (1995) LIGPLOT: a program to generate schematic diagrams of protein–ligand interactions. Protein Eng 8:127–134

Xiang Z, Honig B (2001) Extending the accuracy limits of prediction of side-chain conformations. J Mol Biol 311:421–430

Yang C, Zhang S, He P, Wang C, Huang J, Zhou P (2015) Self-binding peptides: folding or binding? J Chem Inf Model (Epub ahead of print)

Yohe ME, Rossman KL, Gardner OS, Karnoub AE, Snyder JT, Gershburg S, Graves LM, Der CJ, Sondek J (2007) Auto-inhibition of the Dbl family protein Tim by an N-terminal helical motif. J Biol Chem 282:13813–13823

Yohe ME, Rossman K, Sondek J (2008) Role of the C-terminal SH3 domain and N-terminal tyrosine phosphorylation in regulation of Tim and related Dbl-family proteins. Biochemistry 47:6827–6839

Zhou P, Huang J, Tian F (2012) Specific noncovalent interactions at protein–ligand interface: implications for rational drug design. Curr Med Chem 19:226–238

Zhou P, Wang C, Ren Y, Yang C, Tian F (2013) Computational peptidology: a new and promising approach to therapeutic peptide design. Curr Med Chem 20:1985–1996